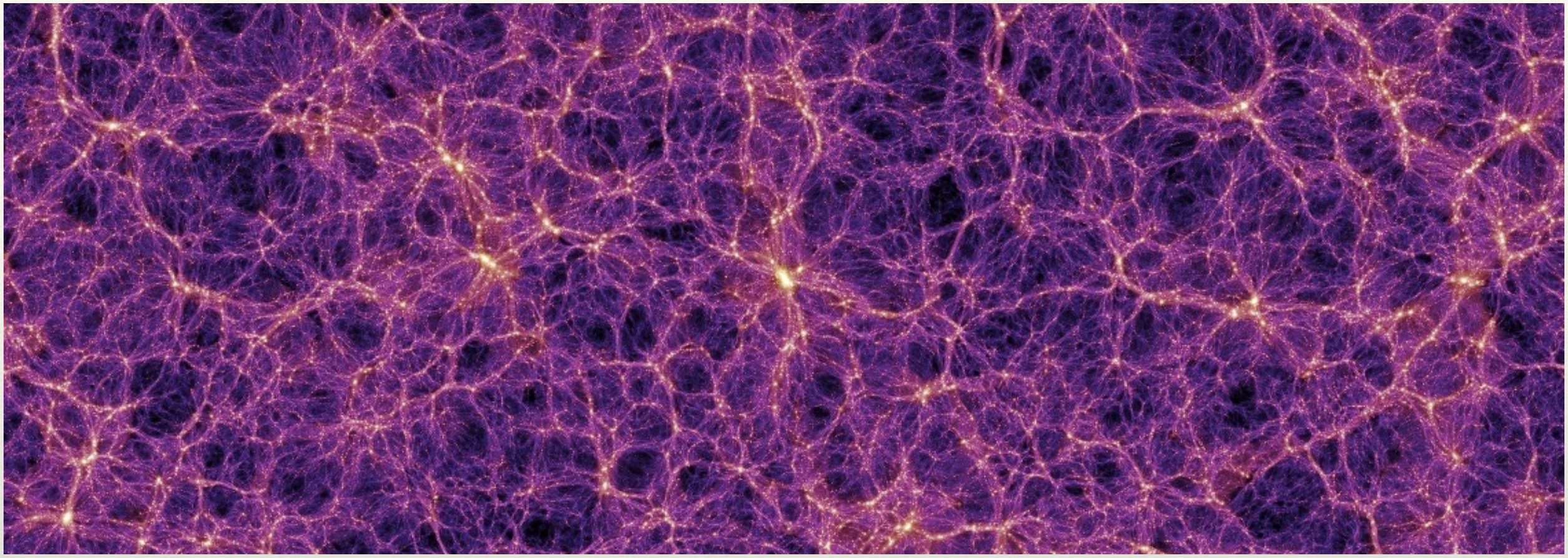

Cristian Cogollos Triviño, on behalf of the RADES group

Results of the Relic Axion Dark-Matter Exploratory Setup (RADES)

Departamento de Física Teórica
Universidad Zaragoza
1542
ICCUB
Institute of Cosmos Sciences
EXCELENCIA MARÍA DE MAEZTU
European Research Council
Established by the European Commission
GOBIERNO DE ESPAÑA
MINISTERIO DE CIENCIA, INNOVACIÓN Y UNIVERSIDADES

32nd Rencontres de Blois in Particle Physics and Cosmology, Blois 19/10/2021

Index

- Dark matter axions (and/or ALPs) and haloscopes
- The RADES setup: Periodic structures for axion detection
- 2018 data taking campaign
- Data analysis and results
- Conclusions and outlook

Dark matter axions and haloscopes

Dark matter axions and haloscopes

What are axions?

- Pseudo Nambu-Goldstone bosons from U(1) SSB introduced for solving strong CP problem
- Electromagnetically neutral pseudoscalars

Can be generalised into

Axion like particles (ALPs):

Neutral Pseudo Nambu-Goldstone bosons from U(1) SSB appearing on several extensions of the Standard Model

Due to their low mass and potentially high abundance, they make good dark matter candidates

(Please, take my word on it, since I don't have much time to spend on this)

Dark matter axions and haloscopes

Axion-photon coupling is present in every model.

$$\mathcal{L}_{a\gamma} = g_{a\gamma\gamma}(\mathbf{E}\cdot\mathbf{B})a$$

$$g_{a\gamma\gamma} = \frac{\alpha_s}{2\pi f_a}\left(\frac{E}{N} - 1.92\right)$$

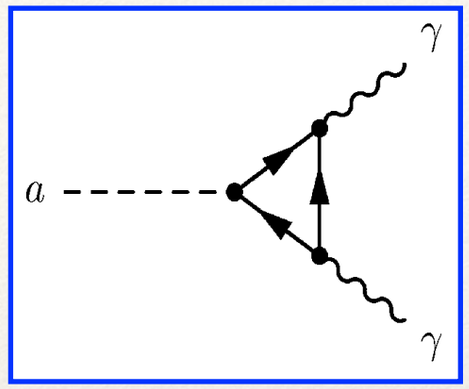

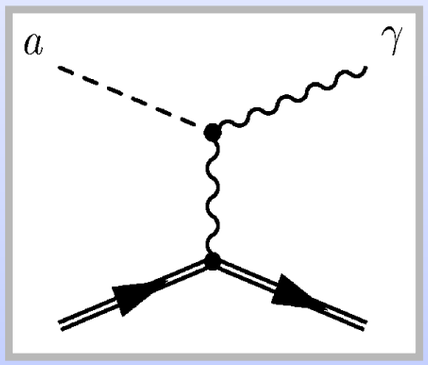

- Axion-photon conversion in the presence of an electromagnetic field (Inverse Primakoff effect)

Probably the most relevant of axion properties for detection purpouses.

Most axion detection strategies are based on the axion-photon coupling

Experimental tests of the invisible axion
P. Sikivie (Phys. Rev. Lett., 51:1415-1417, 1983)

Dark matter axions and haloscopes

A time-varying axion DM field under the influence of a strong magnetic field, can be treated as a classical current source for Maxwell's equations

$$\nabla \cdot \mathbf{E} = 0$$

$$\nabla \times \mathbf{B} - \dot{\mathbf{E}} = g_{A\gamma} \mathbf{B}_e \dot{\mathbf{A}}$$

$$\nabla \cdot \mathbf{B} = 0$$

$$\nabla \times \mathbf{E} + \dot{\mathbf{B}} = 0$$

Dark matter axions and haloscopes

A usual approach to enhance the acquired power from *Axion -> Photon* conversion are resonant cavities

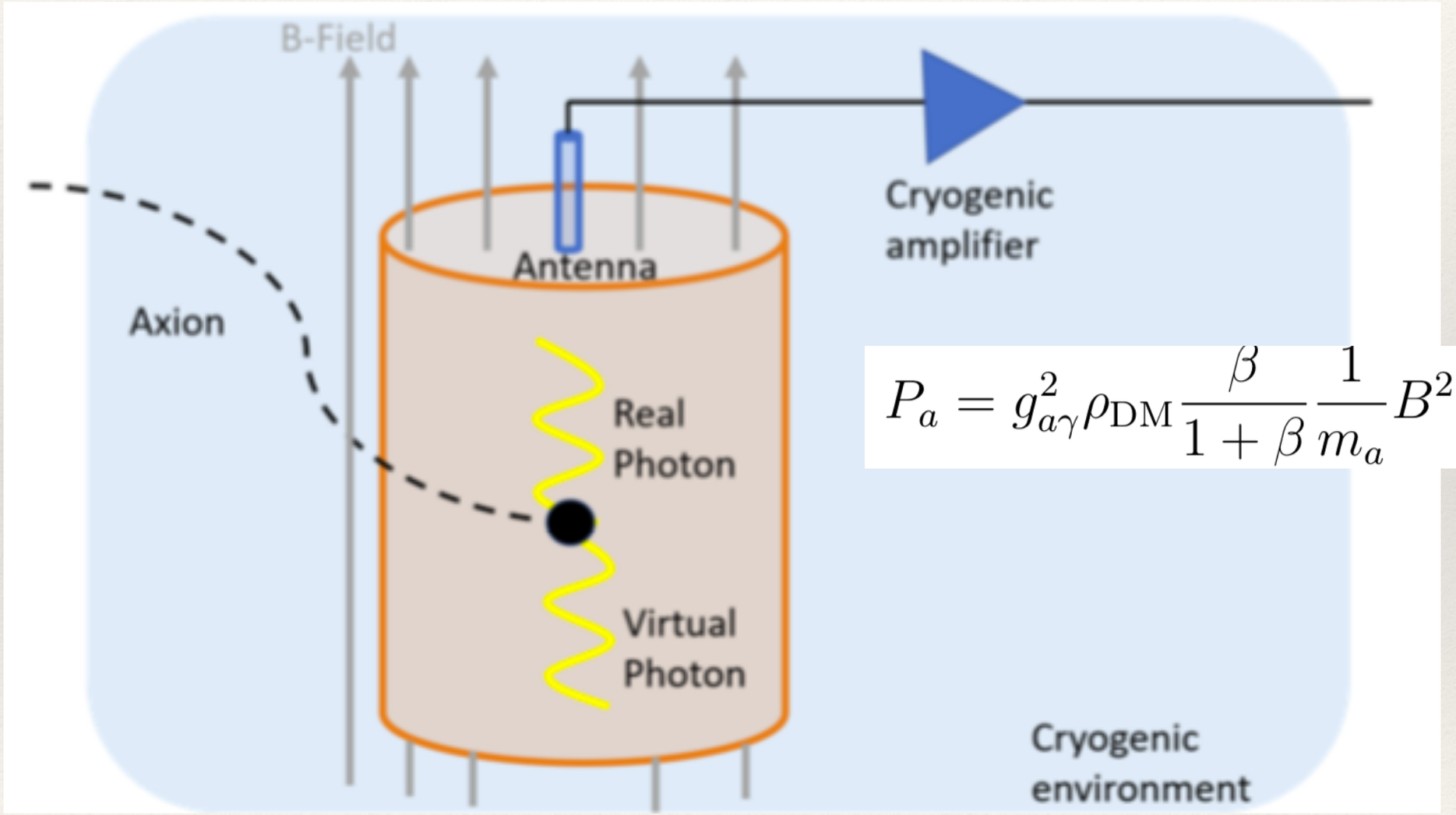

$$P_a = g_{a\gamma}^2 \rho_{\mathrm{DM}} \frac{\beta}{1+\beta} \frac{1}{m_a} B^2 V Q_L G^2$$

Dark matter axions and haloscopes

Exclusion regions for the axion parameter space based on experiments and astrophysical observations have been set during the last decades.

The high part of the RF band is a promising area of the parameter space for DM axions, yet to be studied.

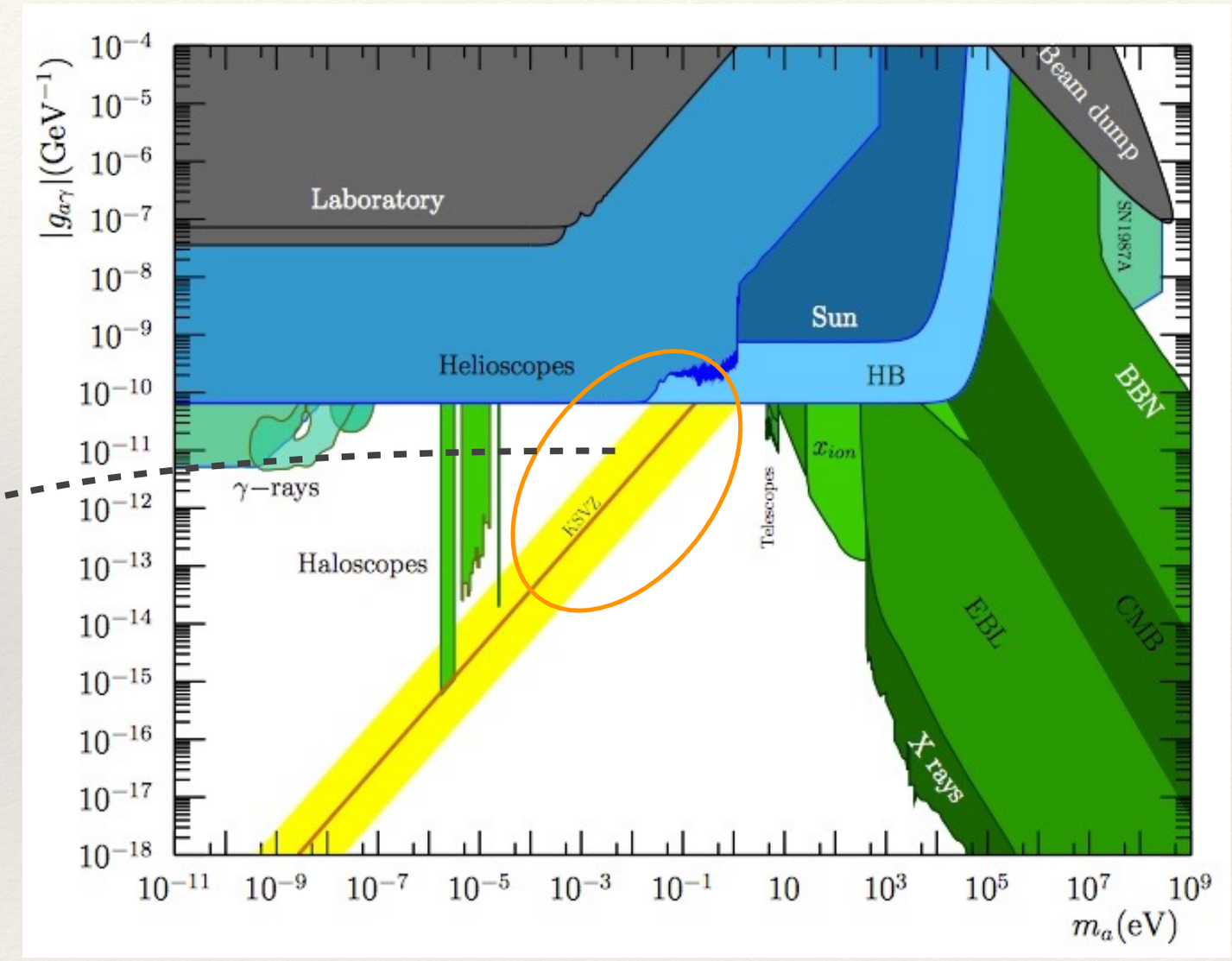

New experimental approaches in the search for axion-like particles
Igor G. Irastorza and Javier Redondo (arXiv:1801.08127)

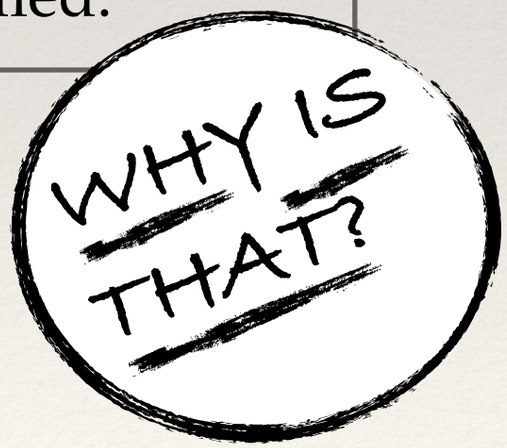

Dark matter axions and haloscopes

Increasing the frequency at which the structure resonates, decreases the volume of the cavity.

Strong inconvenience:

The figure of merit for detection experiments involving haloscopes depends on $B^2VQ^{1/2}$

<u>RADES experiment basis:</u>

A series of cavities connected by irises can behave as a single resonating cavity with all sub-cavities resonating coherently

OUR APPROACH

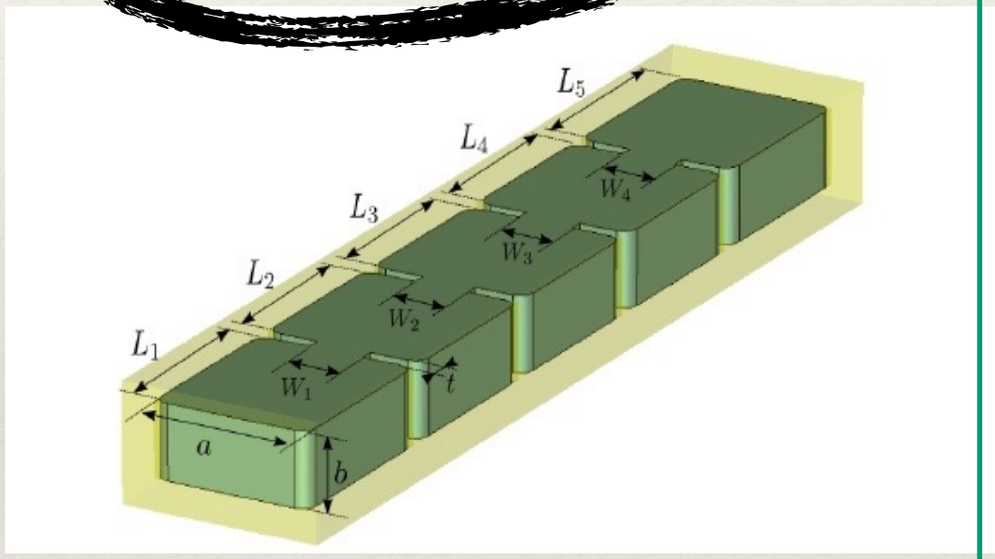

Filter-like structures

Axion Searches with Microwave Filters: the RADES project

A. Alvarez Melcon et al. (arXiv:1803.01243)

The RADES Setup: Periodic structures for axion detection

The RADES Setup: Periodic structures for axion detection

- The electric and magnetic field can be expanded as a sum of orthonormal cavity modes. Using this, Ampere's equation gives the time evolution of the amplitude:

$$\ddot{E}_m + \omega_m^2 E_m + \Gamma_m \dot{E}_m = -g_{A\gamma} B_e \ddot{A} \mathcal{G}_m$$

  - Where the geometric factor G is given by

$$\mathcal{G}_m = \frac{1}{B_e V} \int_{V_e} d^3\mathbf{x}\, \mathbf{B}_e \cdot \mathcal{E}_m$$

- And the losses are parametrised by the gamma factor, defined as:

$$Q_m = \frac{\omega_m}{\Gamma_m}$$

The RADES Setup: Periodic structures for axion detection

Following this theoretical approach we designed our first structure for installing it on one of the bores available at the CAST magnet

Measured Q factor of Q~10^4

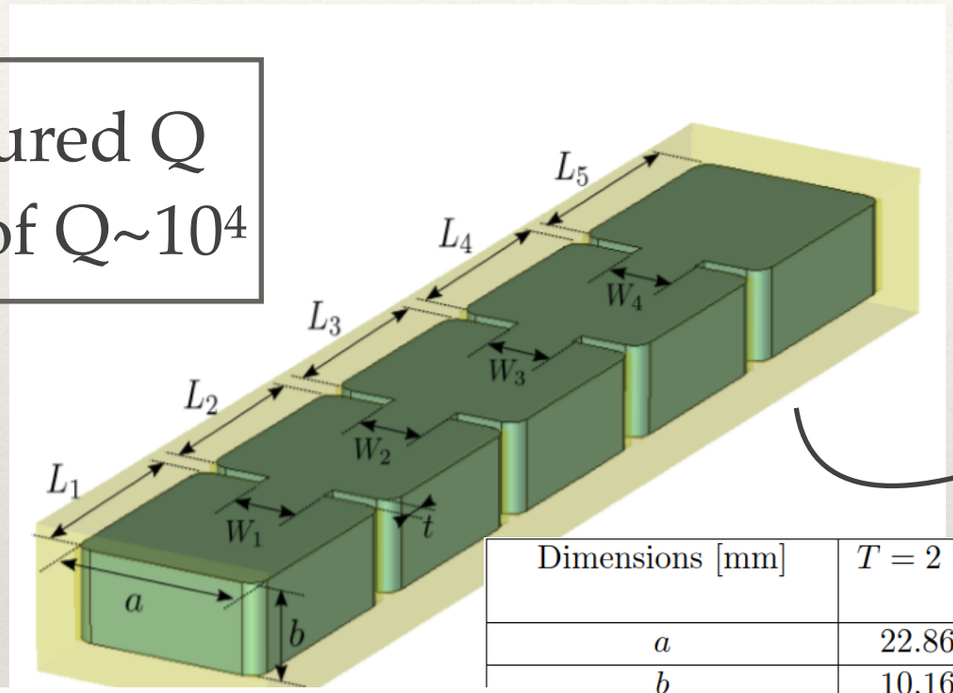

Dimensions [mm]	$T = 2$ K
a	22.86
b	10.16
$L_1 = L_5$	26.68
$L_2 = L_3 = L_4$	25.00
$W_1 = W_2 = W_3 = W_4$	8.00
t	2.00

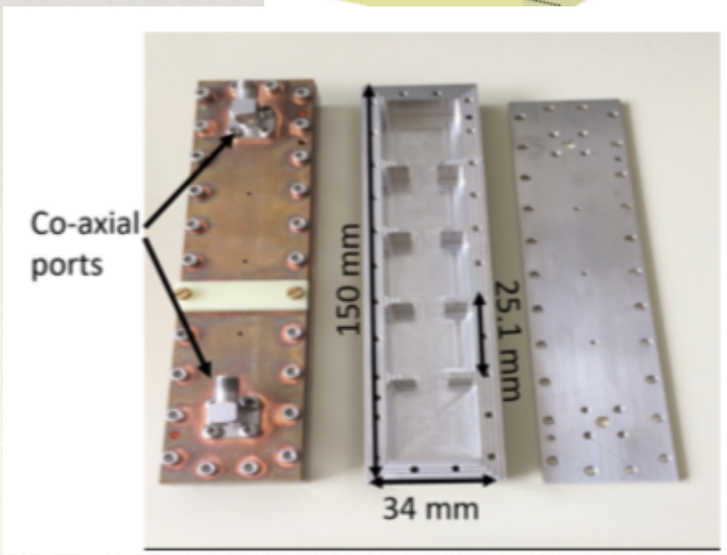

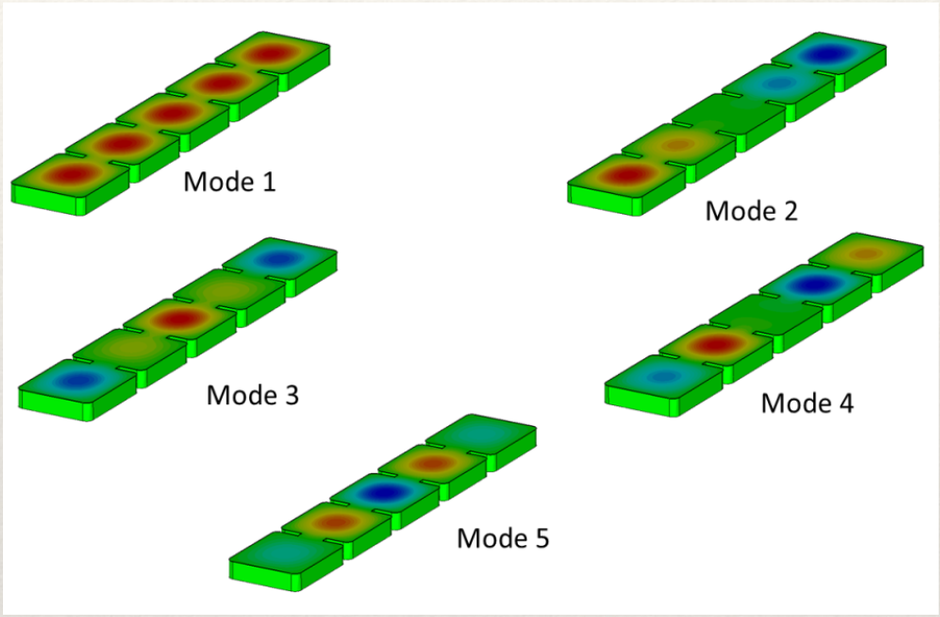

Mode	Electric field pattern $(\text{sign}(\overline{e}_i)_q)$	$\omega_i/2\pi$ (GHz)	$\mathcal{G}_i^2$
1	+ + + + +	8.428	0.65
2	+ + 0 − −	8.454	3.2 10^{-7}
3	− + + + −	8.528	8.1 10^{-5}
4	− + 0 − +	8.625	1.6 10^{-12}
5	− + − + −	8.710	6.4 10^{-6}

Electric field distribution for the five characteristic modes of the structure we designed

The RADES Setup: Periodic structures for axion detection

In 2017 we installed our first cavity inside the CAST magnet for the 2017/2018 data taking campaign

Herr Doktor Sergio Arguedas Cuendis, the real hero. More details can be found on his thesis dissertation, to be made public on the following months.

The RADES Setup: Periodic structures for axion detection

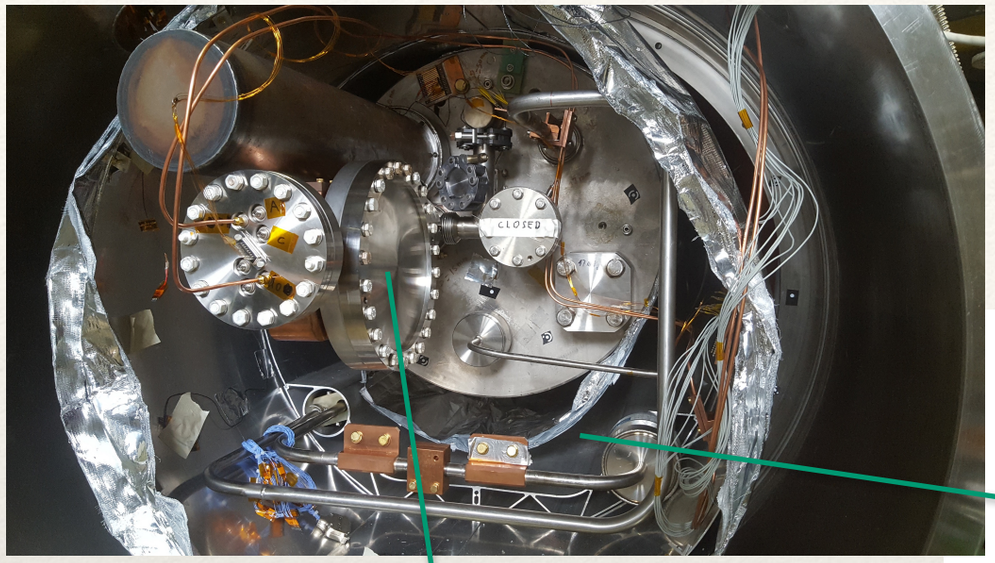

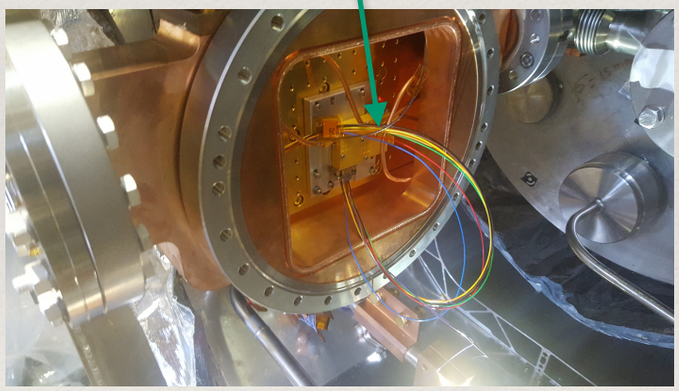

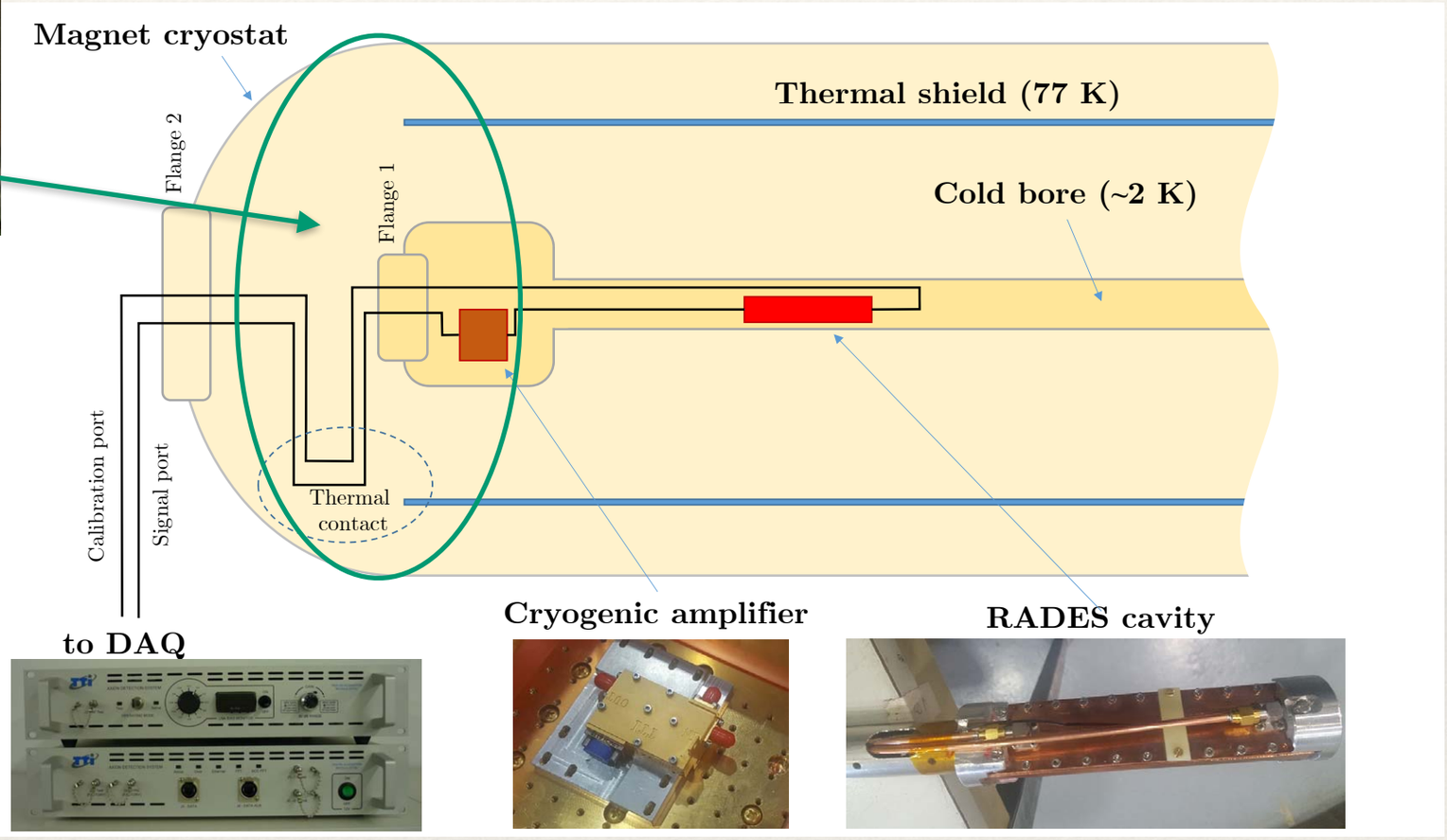

Sketch of the RADES installation from July 2017

2018 Data taking campaign

2018 Data taking campaign

3 Operation circuits:

1. DAQ + 50Ω Load -> Data acquisition
2. DAQ + Noise source -> System temperature measurements
3. VNA -> Coupling and Q-factor measurements

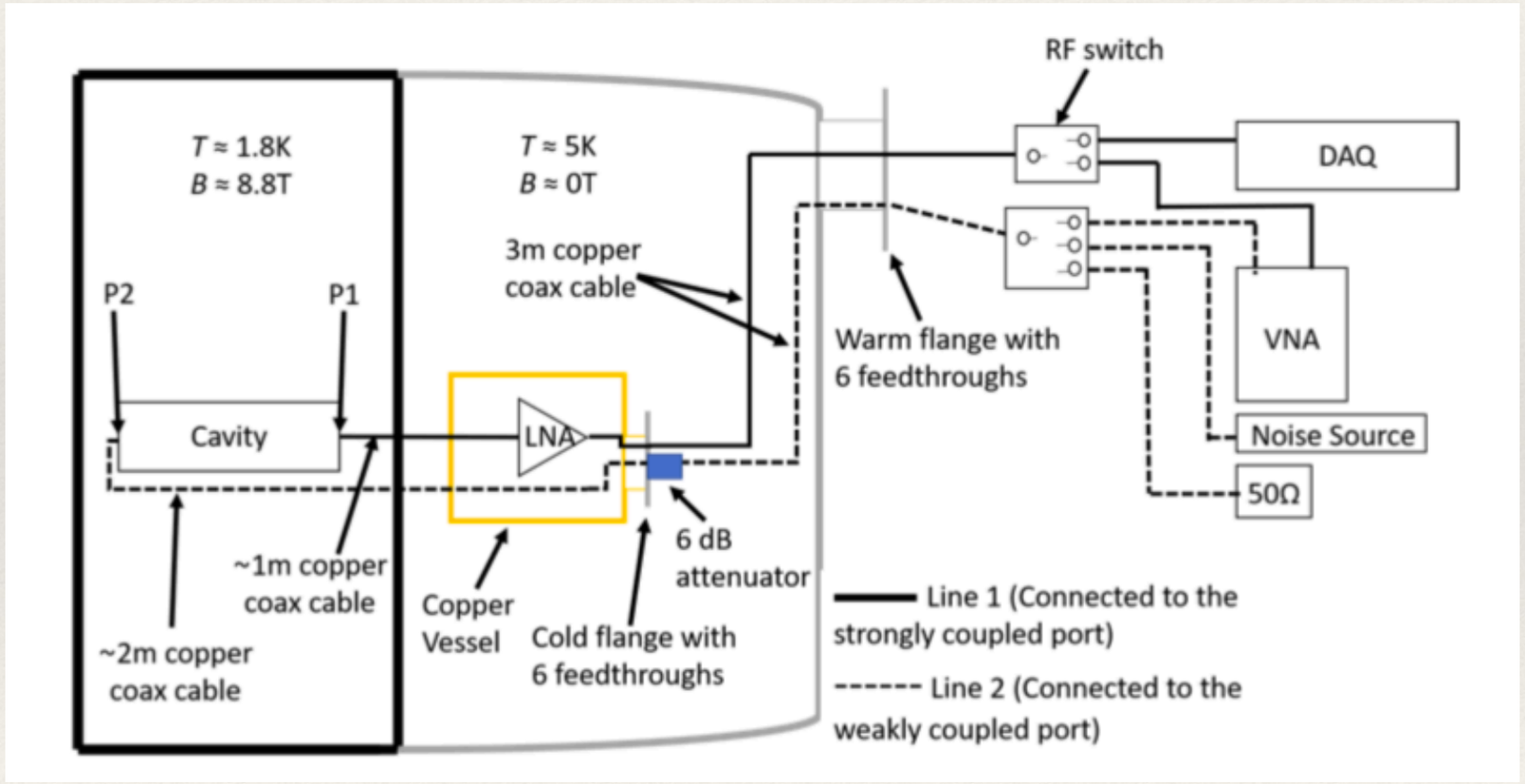

Experimental setup for the 2018 data taking. Including calibration, Q factor and coupling measurement parts.

The RADES Setup: Periodic structures for axion detection

Once the setup was upgraded we could compare the simulations and the measurements for our system with a cleaner signal.

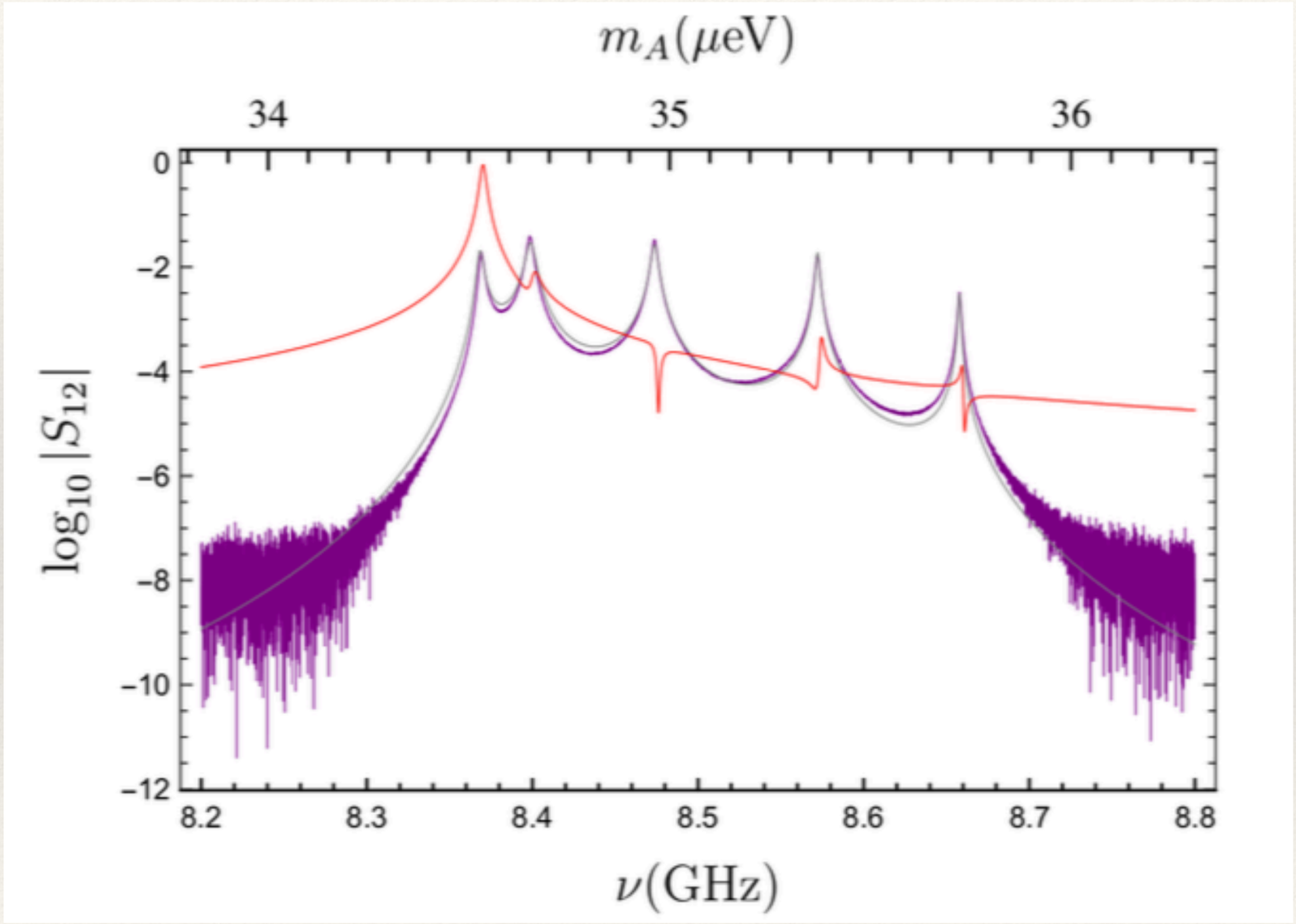

Transmission parameter for theoretical model (gray), axion coupling for the 5 modes (red), measurement for the actual system (purple)

2018 Data taking campaign

- Data acquisition GUI allows for simple checks.
- More robust analysis needed for results.

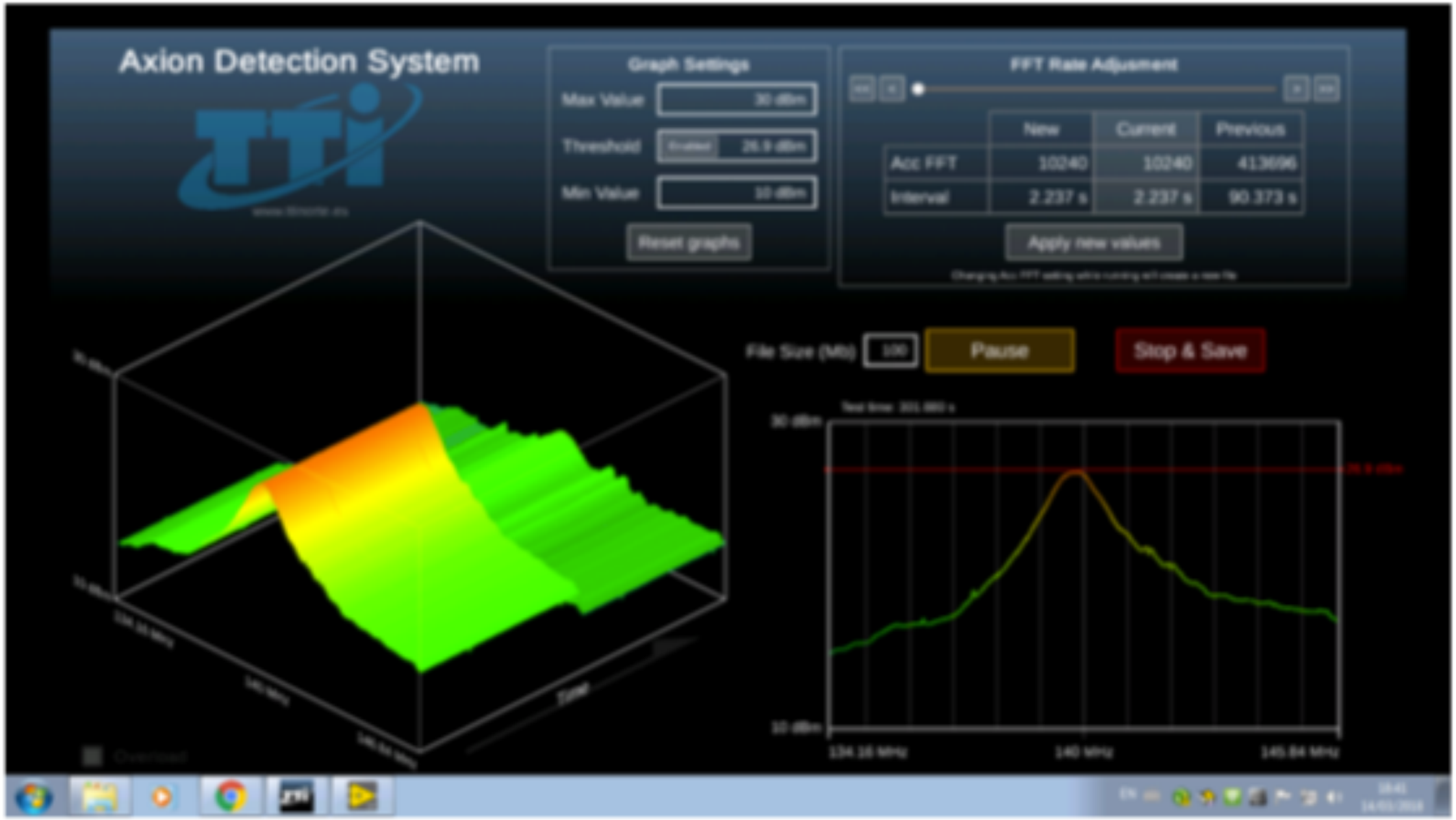

2018 Data taking campaign

- During 2018, coinciding with CAST data taking campaign. The RADES detector took data for 2 months.
- Different local oscillator frequencies were used for handling systematic noise of the data acquisition system.

Magnet-on data		Magnet-off data	
LO freq [GHz]	# of recorded spectra	LO freq [GHz]	# of recorded spectra
8.239	543	8.239	156
8.240	4093	8.240	1203
8.241	1340	8.241	323
8.242	1649	8.242	324
8.243	1144	8.243	0
8.244	2322	8.244	211
8.245	571	8.245	344
8.246	483	8.246	699
8.247	3145	8.247	927
8.248	581	8.248	1047
8.249	1325	8.249	406

Data analysis and results

First results of the CAST-RADES halo scope search for axions at 34.67 μeV

S. Arguedas Cuendis et al. (arXiv: 2104.13798v1)

Data analysis and results

Complications on the analysis:

- Magnet movement introduced complex correlations within datasets generating non-gaussianities on the noise spectra difficult to pinpoint.
- There exists an intrinsic noise structure coming from unknown digitising errors on the FPGA inside the DAQ.
- Existing gain drift of the amplifier.
- Unmeasured variations on the coupling might have happened.
- Temperature of the cables not properly quantified.

Data analysis and results

- Excluding datasets:

	Magnet-on			Magnet-off		
LO freq [GHz]	set #	# of spectra	Date	set #	# of spectra	Date
l_1 : 8.240	1	545	14th Nov.	1	355	14th Nov.
	2	592	15th Nov.	2	334	15th Nov.
	3	627	16th Nov.	3	201	16th Nov.
	4	1745	17th Nov.	4	313	4th Dec.
	5	584	4th Dec.			
$l_{2-\mathrm{on}}$: 8.247	1	576	10th Dec.			
	2	2446	14th Dec.			
	3	124	17th Dec.			
$l_{2-\mathrm{off}}$: 8.248				1	702	6th Nov.
				2	310	6th Nov.
				3	35	9th Dec.

- Magnet-On data: 432 hours -> 103 hours
- Magnet-Off data: 141 hours -> 30 hours

Data analysis and results

- Intrinsic noise structure:

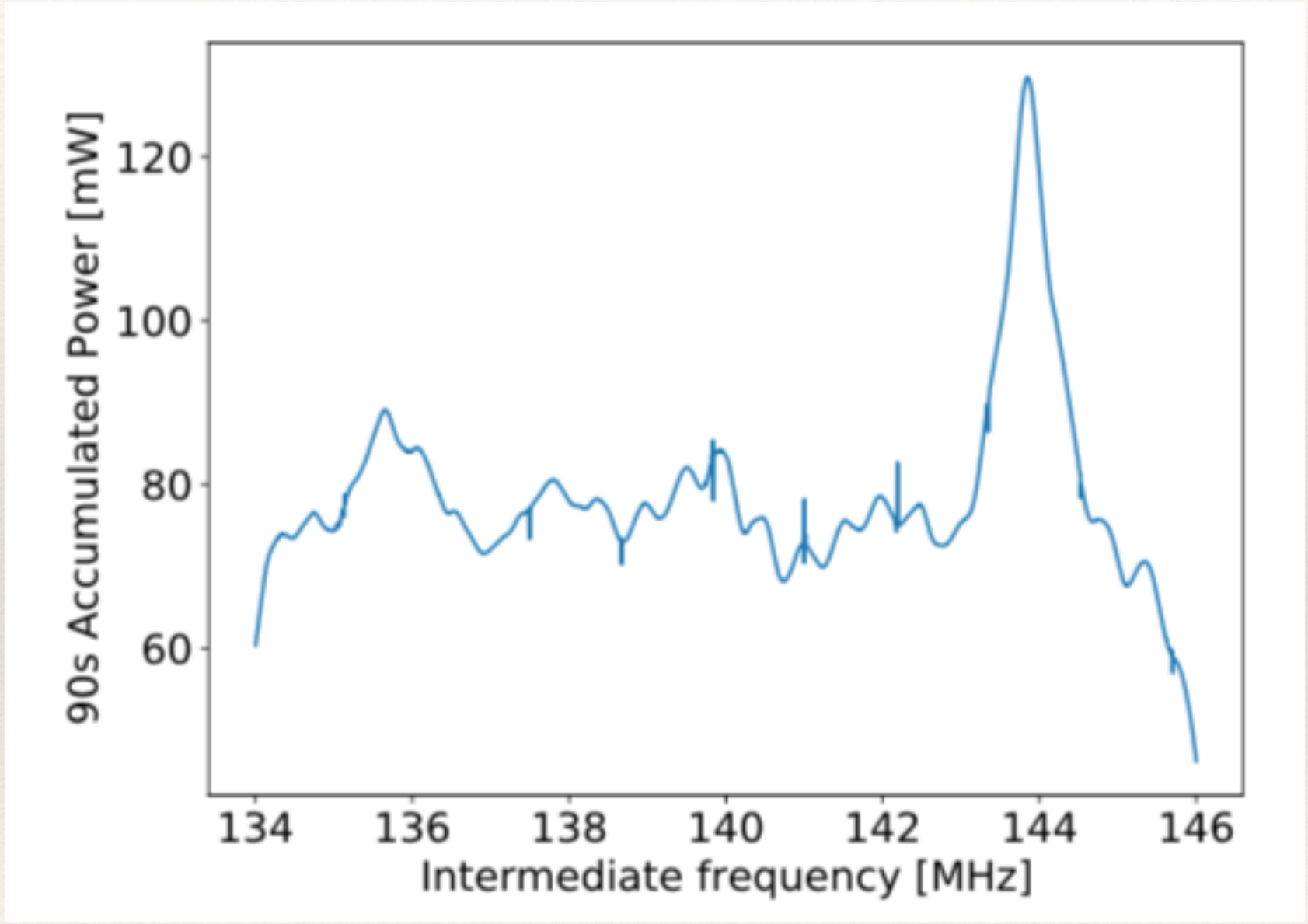

Data analysis and results

- Using two different local oscillator frequencies we can displace the spectrum, keeping the *digital noise* fixed.

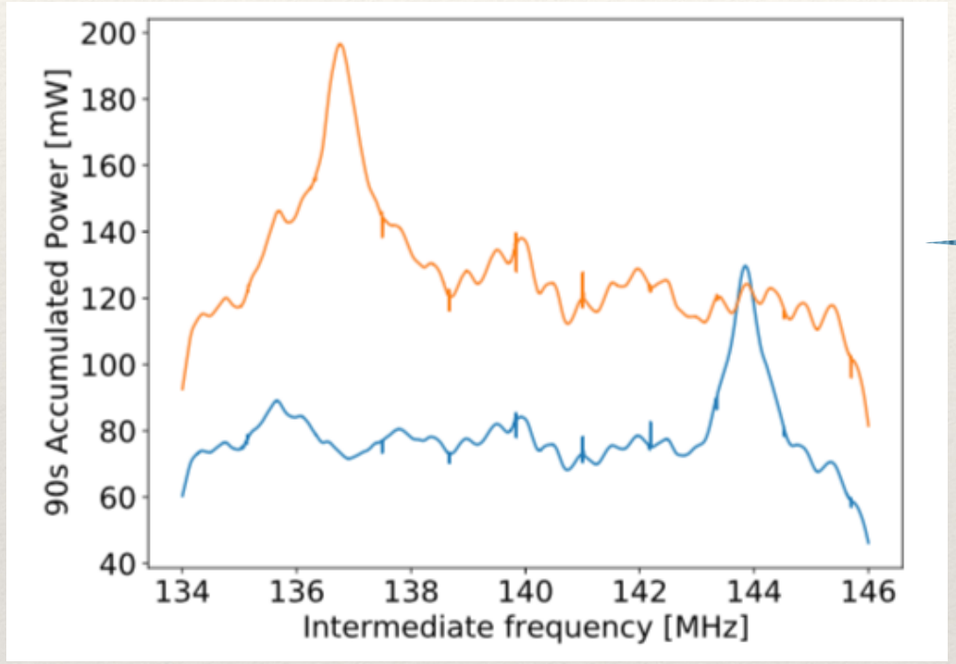

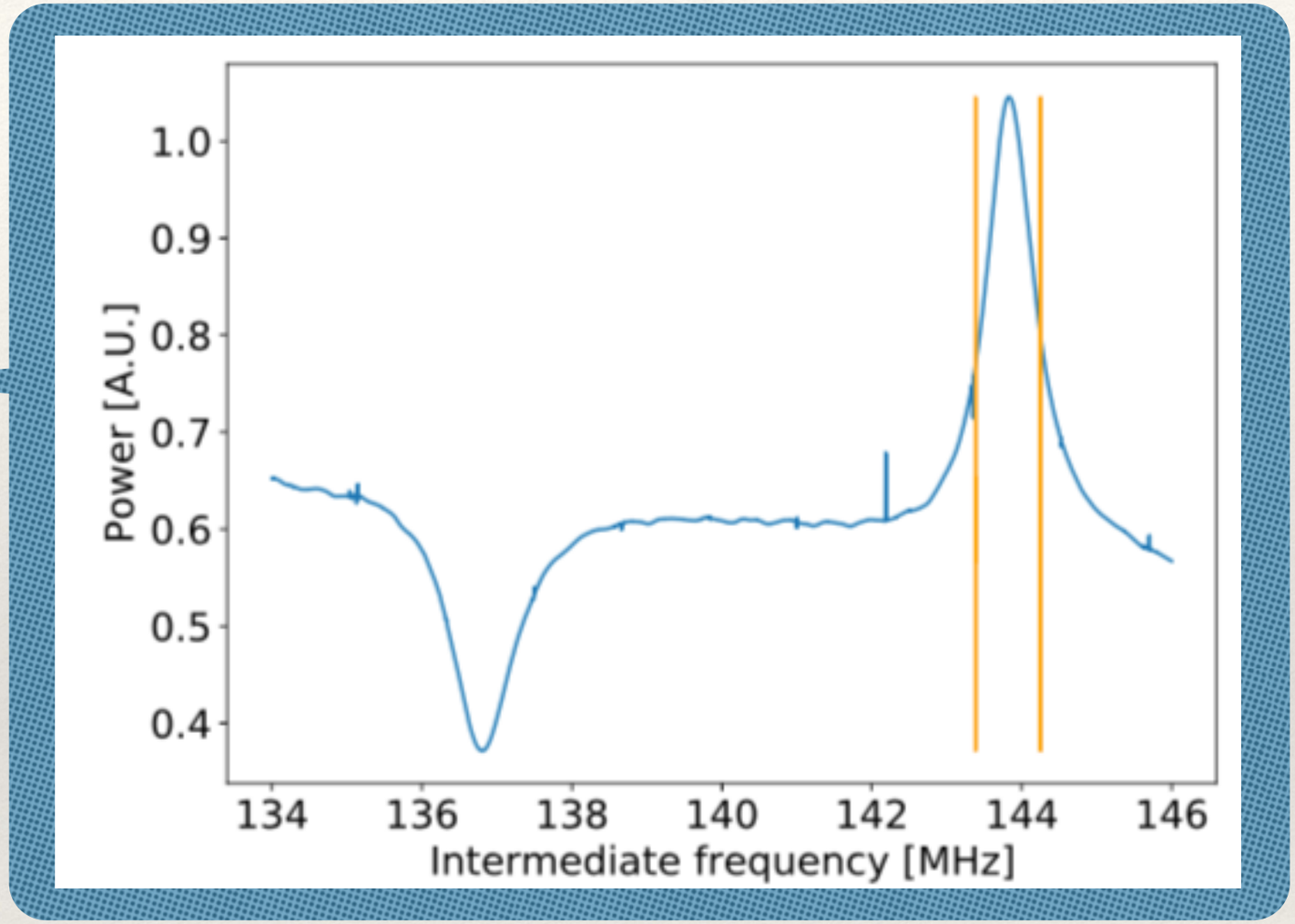

The rest of our analysis is mostly based on the HAYSTAC procedure:

Results from phase 1 of the HAYSTAC microwave cavity axion experiment.

L. Zhong et al. (Phys. Rev. D, 97(9):092001, 2018)

After division of the two spectra, we focus our analysis around the resonance peak.

Data analysis and results

- We compute the mean spectrum and generate a filter function (Savitzky-Golay fit) based on it.
- We divide each dataset by it, to find the power excess w.r.t. mean spectrum.

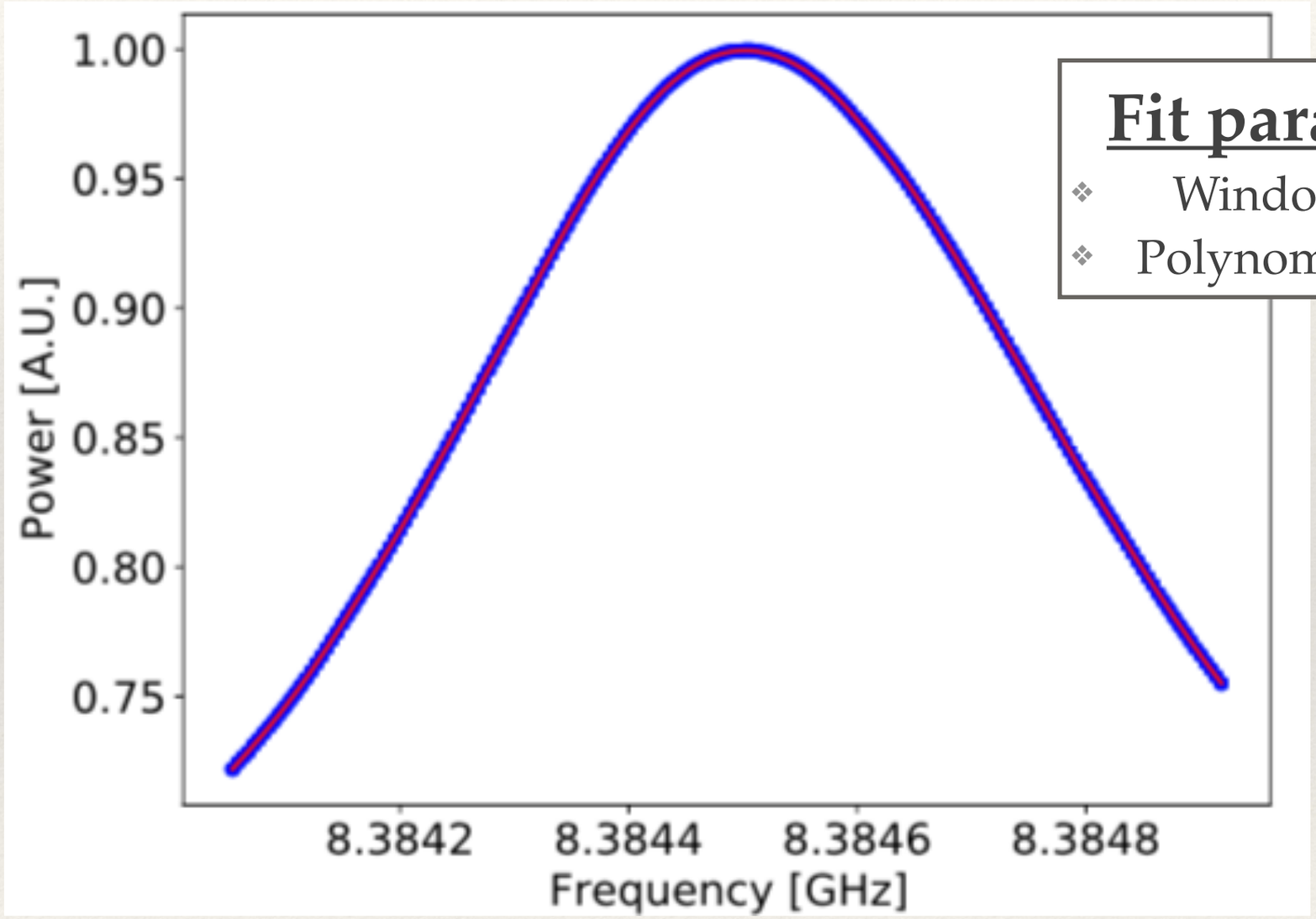

Fit parameters:

- Window size = 15
- Polynomial order = 3

The blue points indicate the data points and the red line the SG-fit produced on the average spectrum.

Data analysis and results

- A second Savitzky-Golay fit was applied to each of the spectra to reduce the effect of the gain drift of the amplifier.

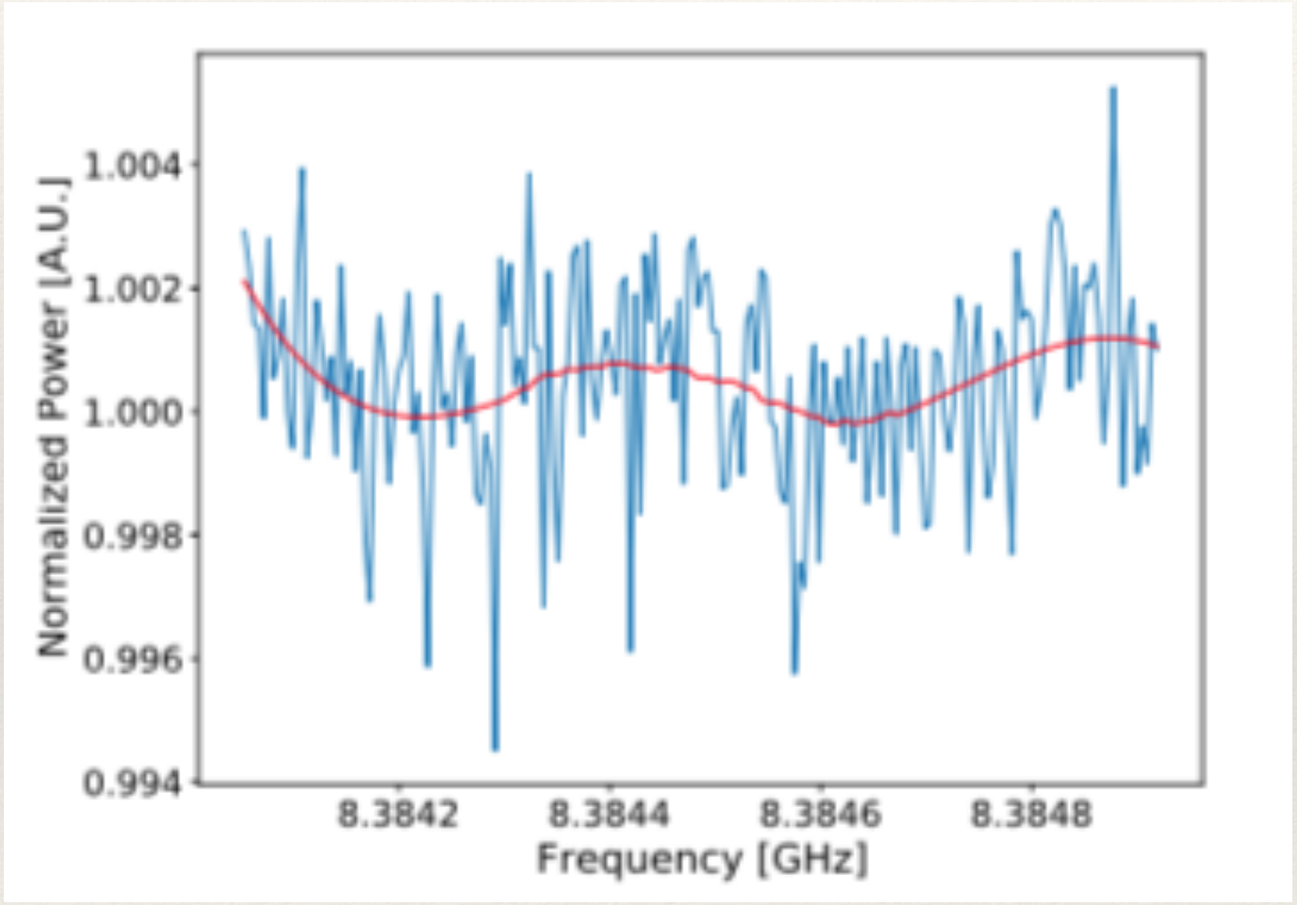

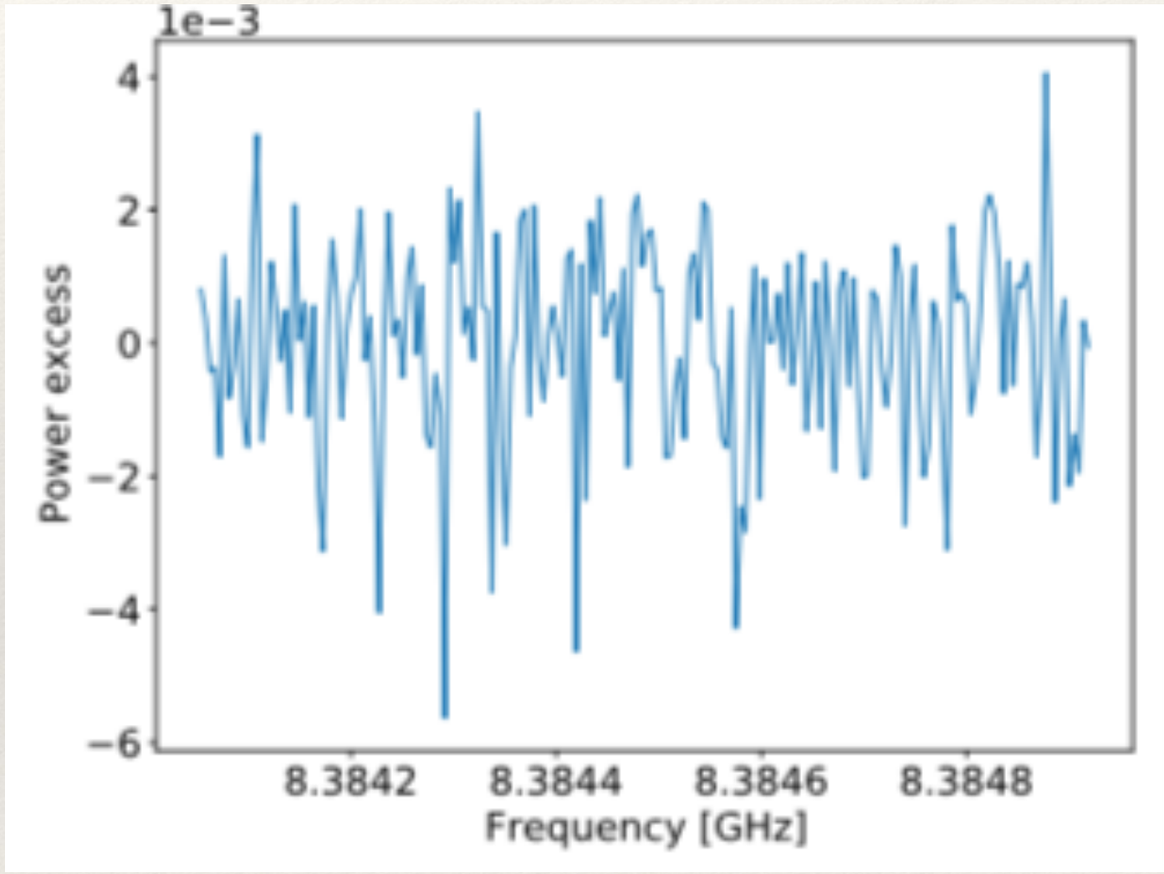

Data analysis and results

- We combine all the spectra in the so called Grand Unified Spectrum.
- Which, in the absence of axions, should follow a gaussian distribution with μ=0, σ=1.

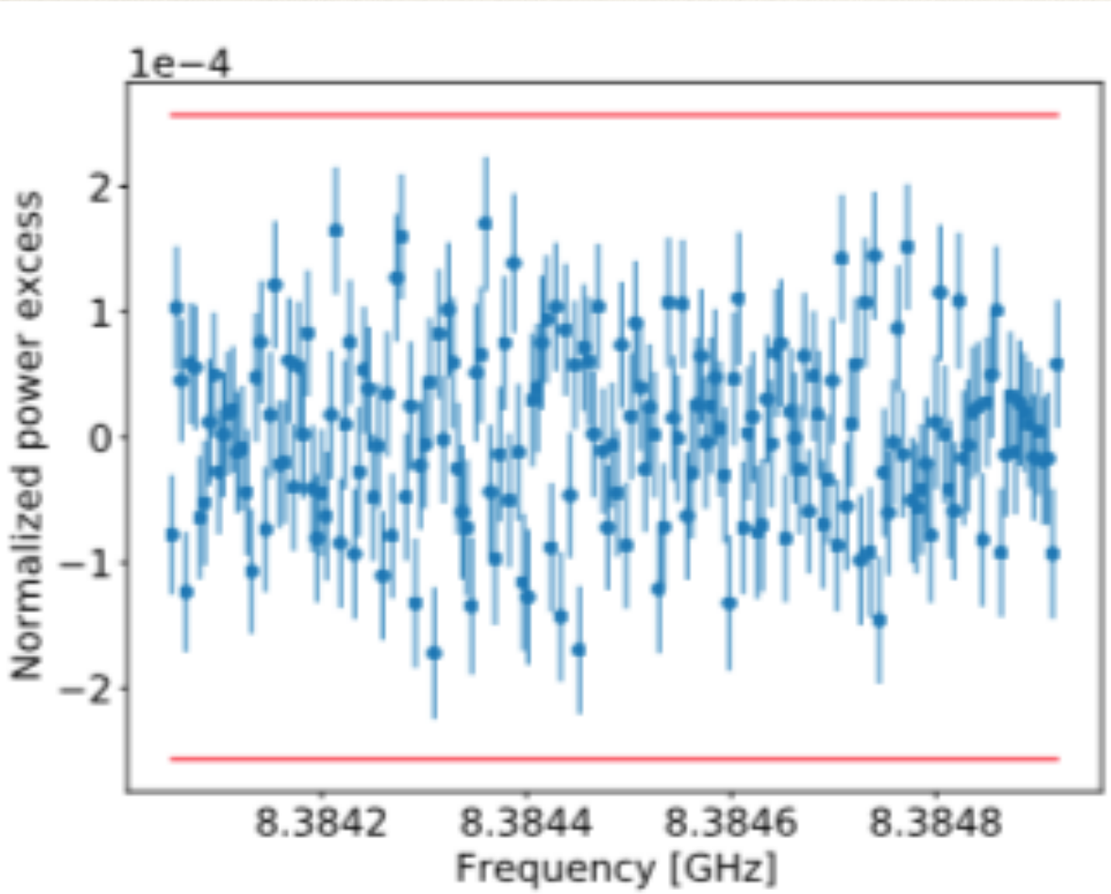

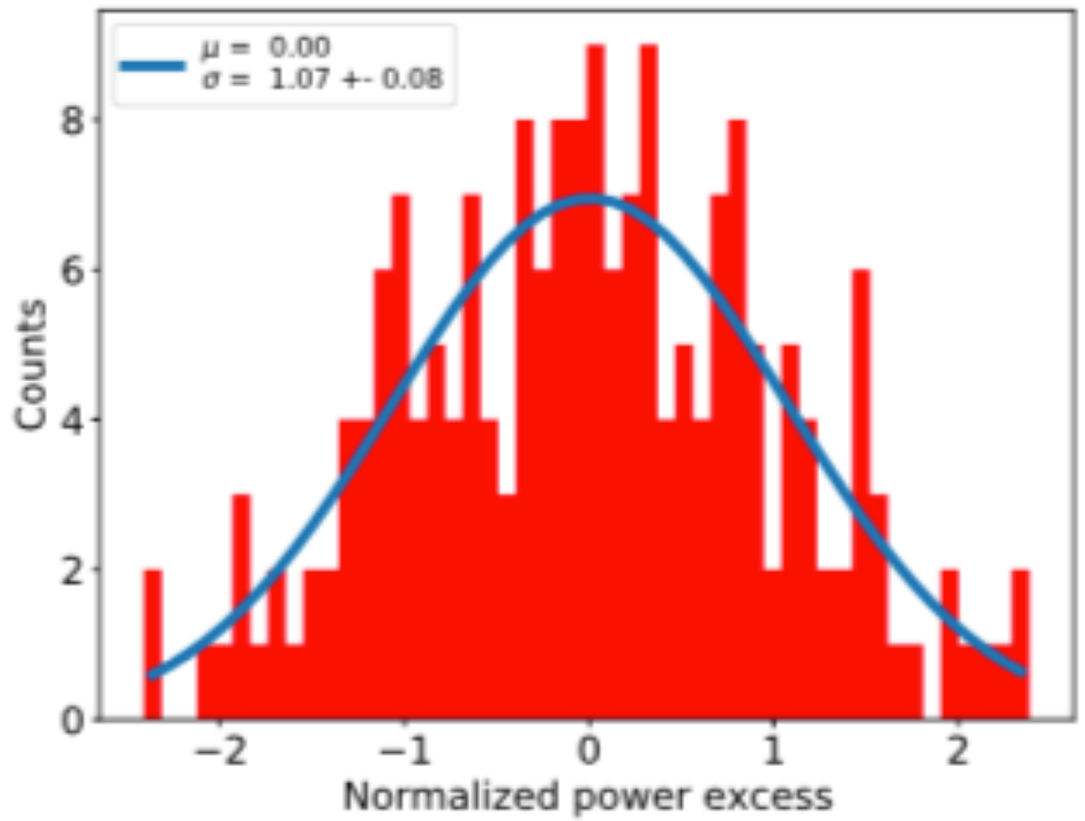

Data analysis and results

- The axion line shape is computed based on the velocity distribution given by the standard isothermal spherical halo model:

$$f(\nu) = \frac{2}{\sqrt{\pi}} \left(\sqrt{\frac{3}{2}} \frac{1}{r} \frac{1}{\nu_a \langle \beta_{MB}^2 \rangle} \right) \sinh \left(3r \sqrt{\frac{2(\nu - \nu_a)}{\nu_a \langle \beta_{MB}^2 \rangle}} \right) \exp \left(-\frac{3(\nu - \nu_a)}{\nu_a \langle \beta_{MB}^2 \rangle} - \frac{3r^2}{2} \right)$$

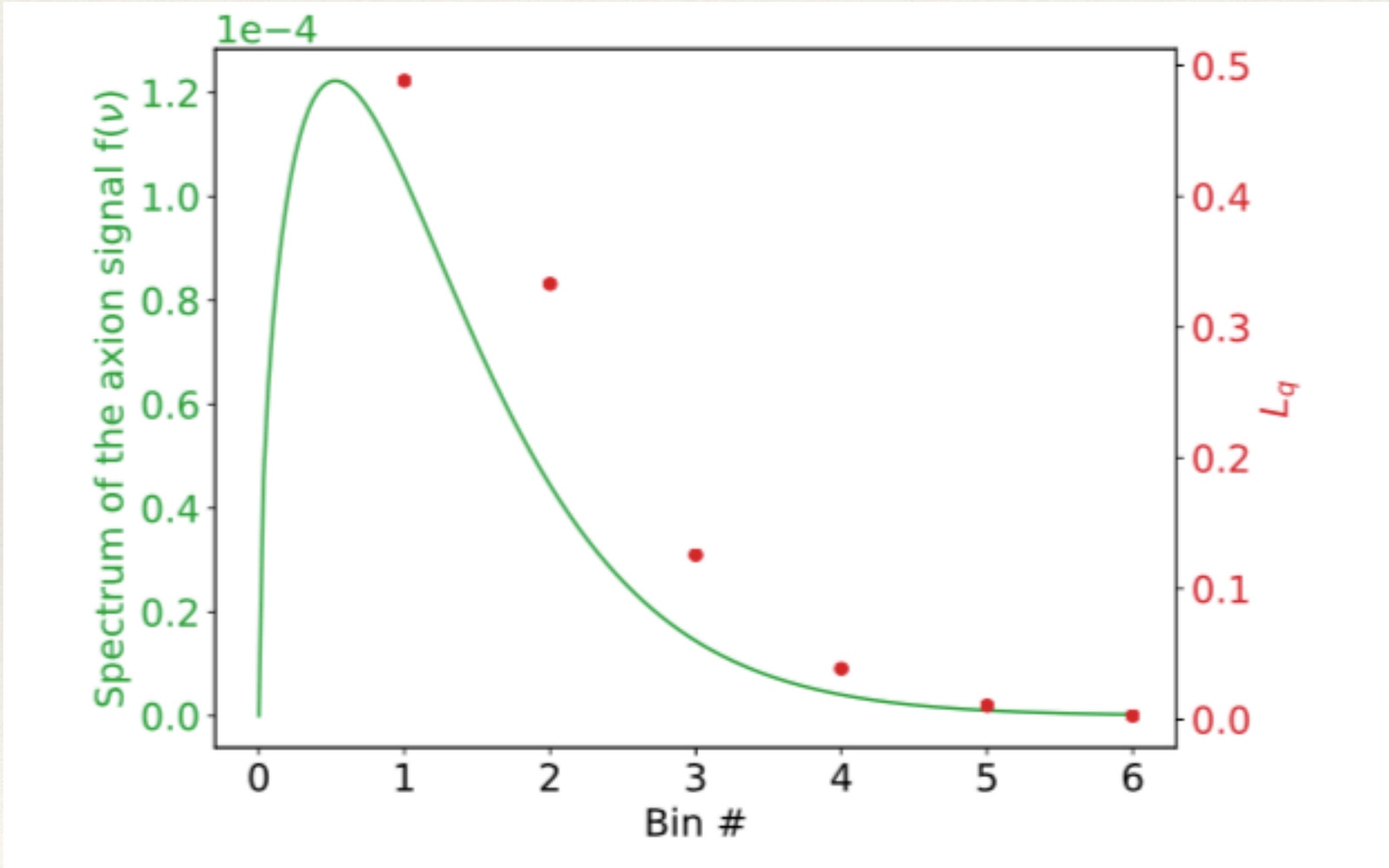

Data analysis and results

- Finally, we perform a likelihood analysis for obtaining an upper limit of the axion power A, given the fit function: $y(x_k^f) = A \cdot L_q^d(x_k^f)$

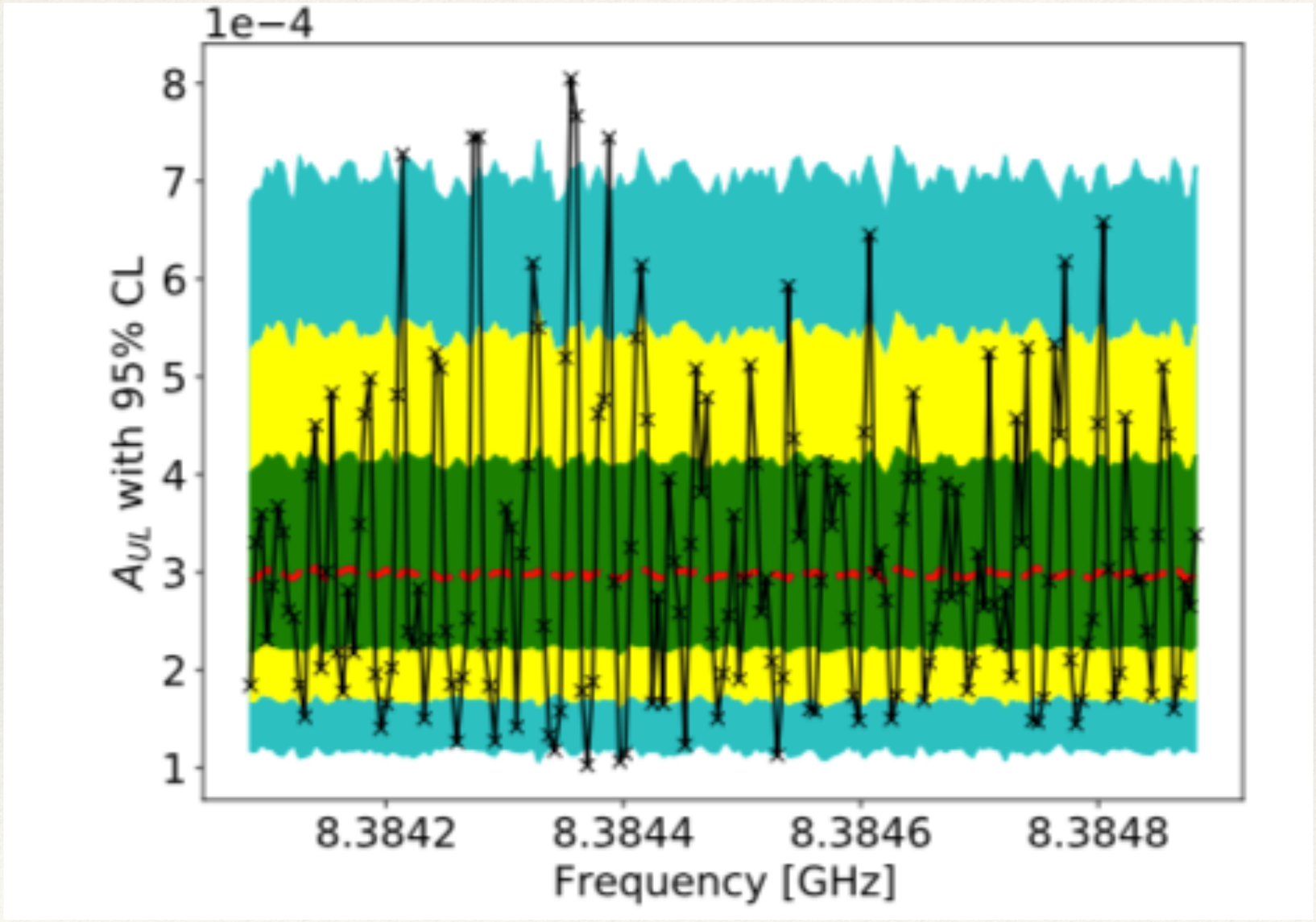

- The red line is computed considering the expected uncertainty, based on integration time and bandwidth.
- The green, yellow and blue areas correspond to 1σ, 2σ and 3σ, respectively.

Data analysis and results

- Based on the analysed data, we generated an exclusion limit around the mass region of 34.67μeV for lower couplings than the current CAST limit.

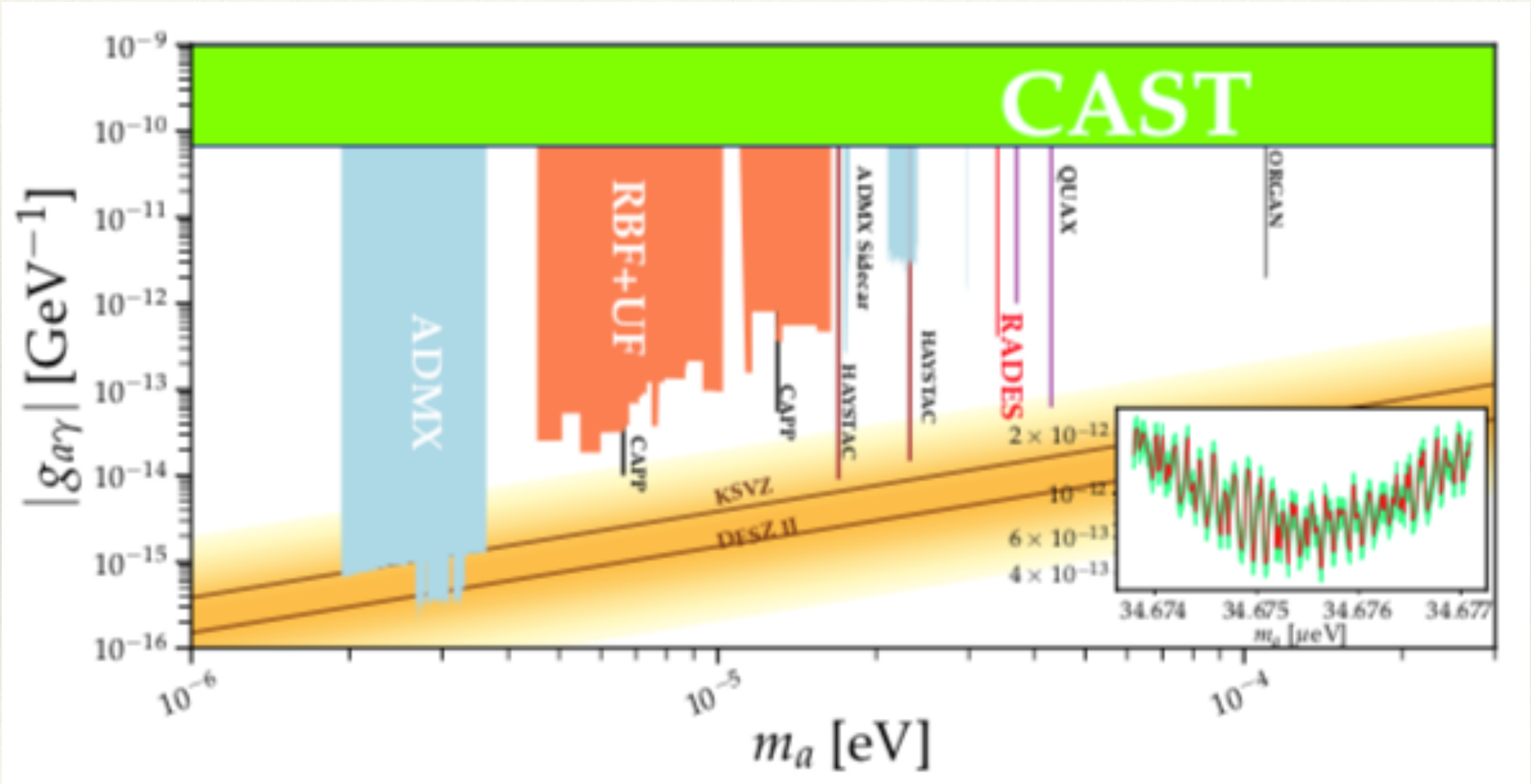

Conclusions and outlook

Conclusions and outlook

- In the RADES group we developed a method for detecting axions at higher frequencies without compromising detection volume.
- We base our approach on an analytical model for a filter with multiple sub-cavities in a formalism that easily introduces axion induced signals.
- Following this model, the first prototype was designed, built and installed at the CAST magnet in 2017, the setup was upgraded for the 2018 data taking campaign.
- Using ~130h of data taking we placed a new limit for axions in the range of 34.674μeV to 34.677μeV.
- New developments are in progress for reaching higher frequencies and implementing a tuning mechanism on our cavities.

Thanks a lot for your attention.

Peace, and keep *sciencing*

Back-up Slides

The RADES Setup: Periodic structures for axion detection

Even though the installation was successful, still there were some improvements to be made before 2018 data taking:

- We had to substitute the feedthroughs that connect our system to the exterior to get rid of extra reflections we were having.
- We added an extra test port for our cryogenic amplifier
- We attenuated the insertion port of our cavity to reduce our noise temperature

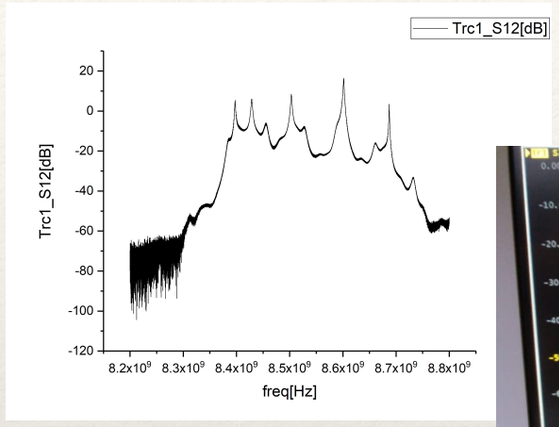

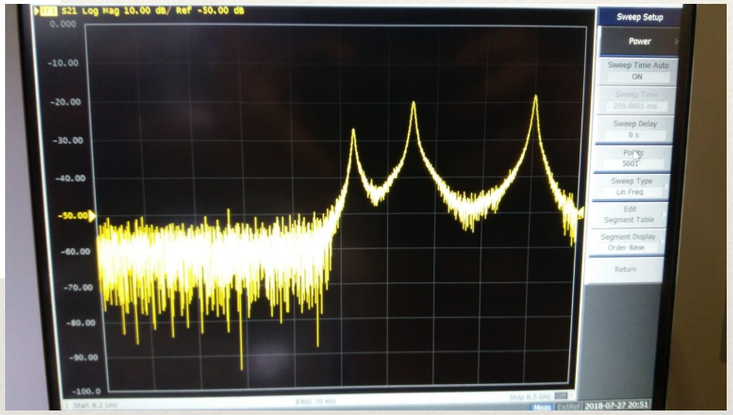

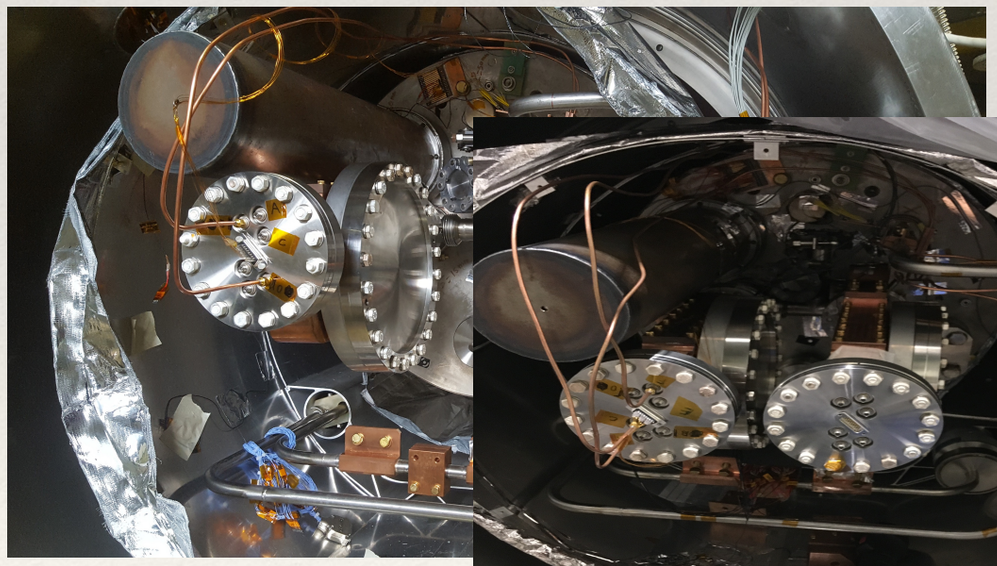

Back-up: Periodic structures for axion detection

- The electric and magnetic field can be expanded as a sum of orthonormal cavity modes. Using this, Ampere's equation gives the time evolution of the amplitude:

$$\ddot{E}_m + \omega_m^2 E_m + \Gamma_m \dot{E}_m = -g_{A\gamma} B_e \ddot{A} \mathcal{G}_m$$

  - Where the geometric factor G is given by

$$\mathcal{G}_m = \frac{1}{B_e V} \int_{V_e} d^3\mathbf{x}\, \mathbf{B}_e \cdot \mathcal{E}_m$$

- And the losses are parametrized by the gamma factor defined as:

$$Q_m = \frac{\omega_m}{\Gamma_m}$$

Back-up:

Periodic structures for axion detection

For the design of our structures in particular we will assume the following:

- We will consider a number of N cavities coupled through small irises through which they exchange EM energy.
- For these cavities we will consider similar geometries and thus a similar fundamental mode at a common frequency for all.
- Finally, we will consider a linear coupling between the different cavities q and q', described with a coupling coefficient $K_{qq'}$

With this in mind we can build the following model for the axion-cavity energy coupling

Back-up:

Periodic structures for axion detection

- When excited by a monochromatic axion DM field, the system of coupled equations for the amplitude is given by:

$$\left(\omega^2\mathbb{I} - \mathbb{M}\right)\bar{\Xi} = \bar{J}_A = -g_{A\gamma}B_e A_0 \omega^2 \bar{\mathcal{G}}$$

- Where Ξ is a vector containing the E-field amplitudes
- And the M matrix contains the natural frequencies, damping factors and coupling between the cavities:

$$\mathbb{M} = \begin{pmatrix} \tilde{\Omega}_1^2 & K_{12} & 0 & 0 & 0 & 0 \\ K_{21} & \tilde{\Omega}_2^2 & K_{23} & 0 & 0 & 0 \\ 0 & K_{32} & \tilde{\Omega}_3^2 & K_{34} & 0 & 0 \\ 0 & 0 & \ddots & \ddots & \ddots & 0 \\ 0 & 0 & 0 & \ddots & \ddots & \ddots \\ 0 & 0 & 0 & 0 & K_{N,N-1} & \tilde{\Omega}_N^2 \end{pmatrix}$$

Back-up:

Periodic structures for axion detection

The results of diagonalizing the previous matrix have a straightforward physical interpretation:

- The eigenvalues correspond to the square of the N resonant eigenfrequencies of the given EM filter.

- The eigenvectors represent the E-field amplitude and phase of the fundamental mode of each of the individual cavities.

Back-up:

Periodic structures for axion detection

If we now restrict ourselves to the study of a structure composed by 5 subcavities

- For a given eigenvalue ω^2_i, the problem leads to the following system of linear equations.

$$\omega_i^2 \begin{pmatrix} e_{i1} \\ e_{i2} \\ e_{i3} \\ e_{i4} \\ e_{i5} \end{pmatrix} = \mathbb{M} \begin{pmatrix} e_{i1} \\ e_{i2} \\ e_{i3} \\ e_{i4} \\ e_{i5} \end{pmatrix} = \begin{pmatrix} \Omega_1^2 e_{i1} + K_{12} e_{i2} \\ K_{12} e_{i1} + \Omega_2^2 e_{i2} + K_{23} e_{i3} \\ K_{23} e_{i2} + \Omega_3^2 e_{i3} + K_{34} e_{i4} \\ K_{34} e_{i3} + \Omega_4^2 e_{i4} + K_{45} e_{i5} \\ K_{45} e_{i4} + \Omega_5^2 e_{i5} \end{pmatrix}$$

- Let's emphasize that we can choose the design parameters Ω and K by altering the dimensions of the cavities and irises.

Back-up:

Periodic structures for axion detection

- We have chosen to fix a desired characteristic frequency ω_i and design a filter that maximizes the geometric factor for that frequency.
- The simplest solution is to take all coupling coefficients to be equal to a fixed value k, which gives the following solution for the individual cavity frequencies:

$$\Omega_2^2 = \Omega_3^2 = \Omega_4^2 = \omega_1^2 \left(1 - 2k^{(1)}\right) \qquad \Omega_1^2 = \Omega_5^2 = \omega_1^2 \left(1 - k^{(1)}\right)$$

- All cavities must share the same resonant frequency, except the first and last one.
- Once we have fixed those values we can compute the associated dimensions of the corresponding structure.

Data analysis and results

- Transfer function of different SG filters for the region of interest

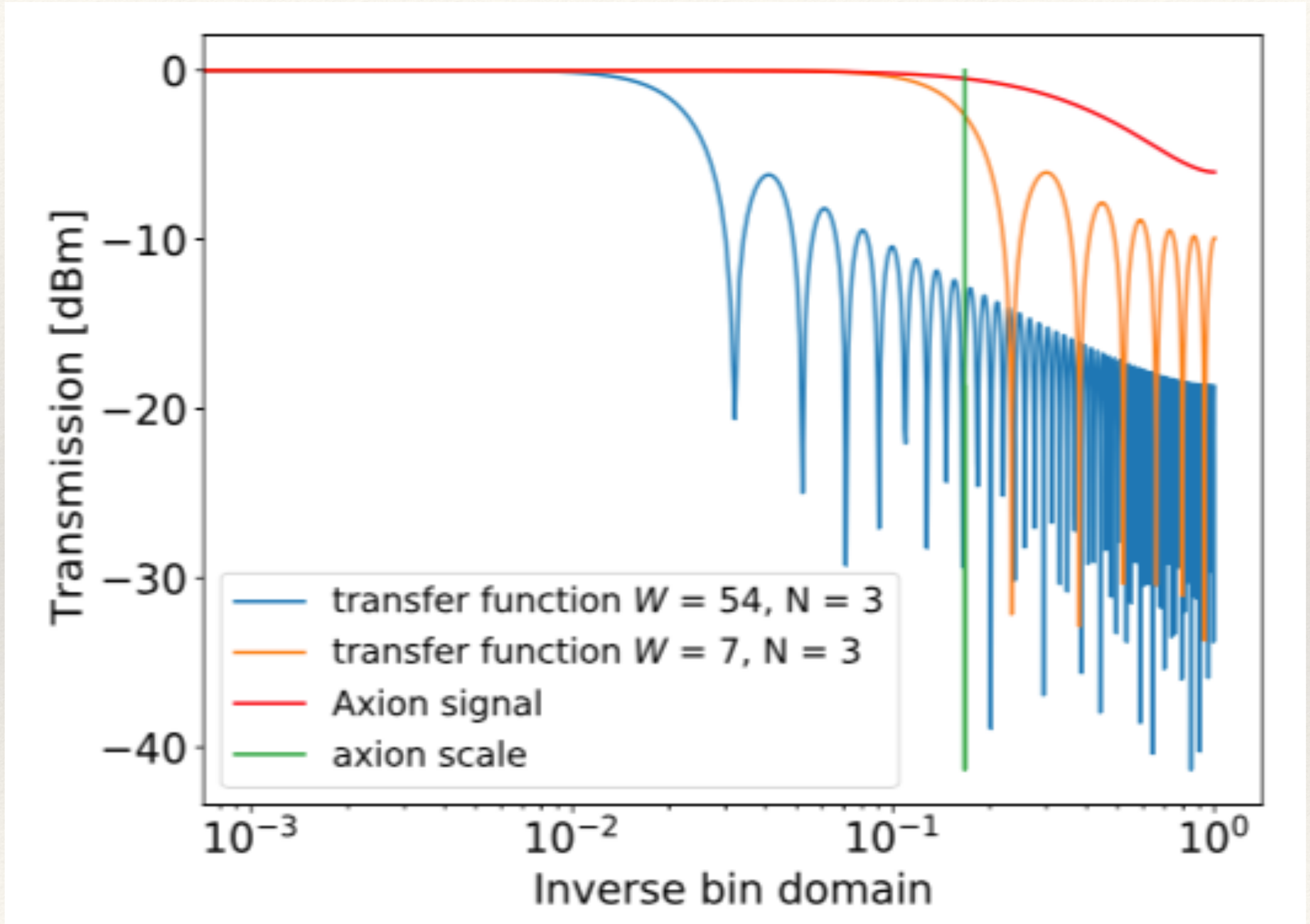

Data analysis and results

- The axion line shape was “deformed” for performing the analysis, taking into account effects arising from the Savitzky-Golay filters applied to the data.

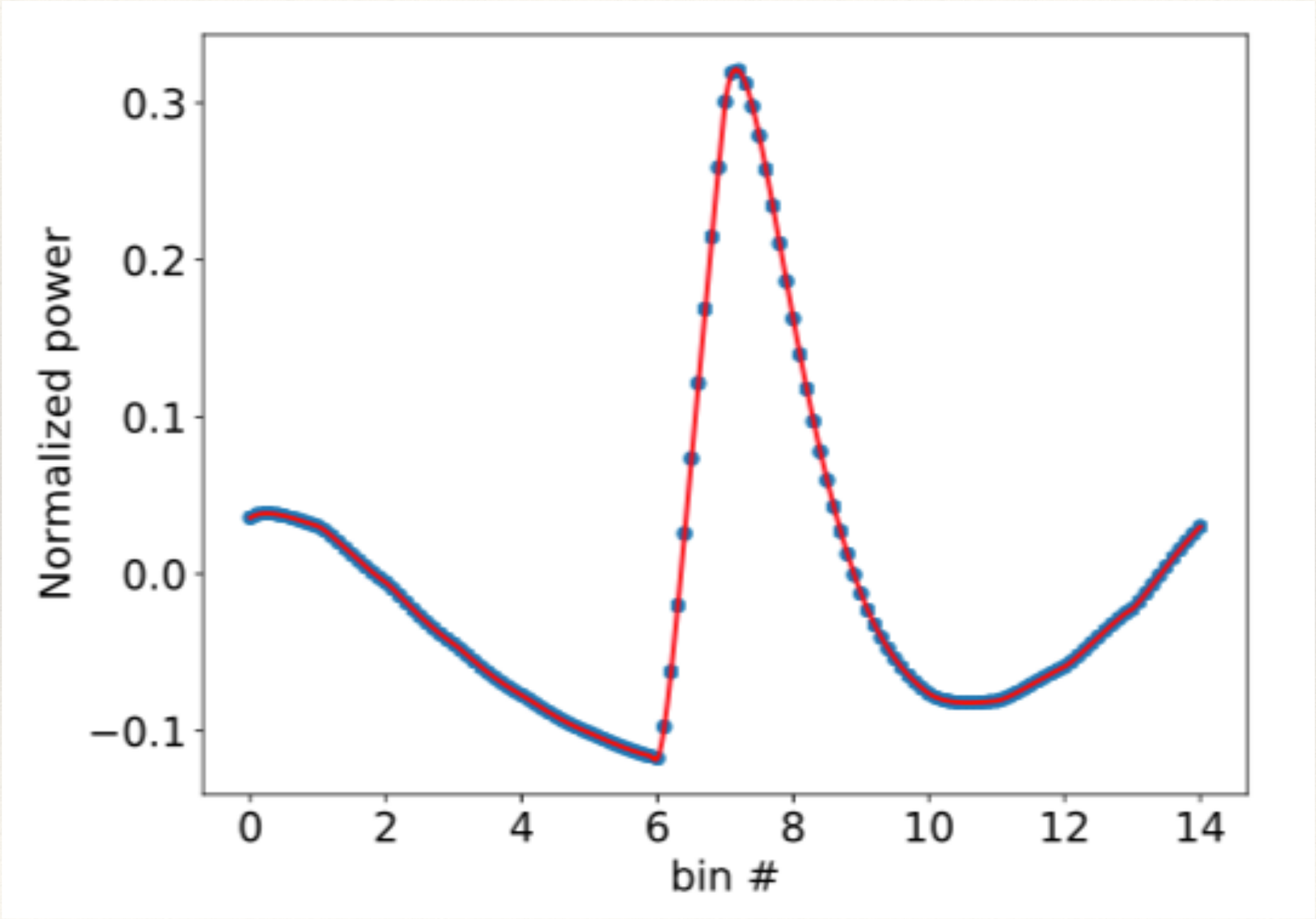

Data analysis and results

Parameters for the exclusion limits:

$$P_a = g_{a\gamma}^2 \rho_{\mathrm{DM}} \frac{\beta}{1+\beta} \frac{1}{m_a} B^2 V Q_L G^2$$

$$P_a = A_{UL} \cdot P_N = A_{UL} k_b T_{sys} \Delta\nu$$

Parameter	Value
$\Delta\nu$	4577 Hz
T_{sys}	(7.8 ± 2.0) K
Q_L	11009 ± 483
β	0.50 ± 0.11
B	(8.8 ± 0.0088) T
ρ_{DM}	$0.45\,\mathrm{GeVcm}^{-3}$
G^2	0.65
Volume	0.03 L
η	0.83